

Rovers for Intelligent, Agile Traverse of Challenging Terrain

P. Schenker, T. Huntsberger, P. Pirjanian
Jet Propulsion Lab., Calif. Institute of Technology
4800 Oak Grove Drive/MS 198-219
Pasadena, CA 91109
paul.s.schenker@jpl.nasa.gov
<http://prl.jpl.nasa.gov>

S. Dubowsky, K. Iagnemma, V. Sujan
Department of Mechanical Engineering
Massachusetts Institute of Technology
Cambridge, MA 02139
dubowsky@mit.edu
<http://robots.mit.edu/>

Abstract

Planetary surface mobility has to date been limited to benign locations. If rover systems could be developed for more challenging terrain, e.g., sloped and irregularly featured areas, then planetary science opportunities would be greatly expanded. We have in the last several years carried out a related program of R&D that involves new concepts in reconfigurable mobility and on-board adaptive control of same in response to the sensed and changing environment. Several prototype systems and their in-field demonstration have resulted, including a single "All Terrain Explorer" which significantly extends operability into steeply sloped sandy terrain, as well as a new "Cliff-bot" which achieves near vertical cliff-side operation via fully distributed sensing and control within a team of cooperative agents. We overview these developments, noting their potential for a broader class of robotic system applications.

1. Introduction

Autonomous mobility over rough and hard-to-access terrain is a topic of both technical and applications interest in robotics. The technical challenges are considerable, as they span issues in mechanical design, sensing, planning, control, and underlying models and simulation of same. The potential applications are broad, one being rovers for the scientific exploration of solar system bodies (planets, moons, asteroids) with disparate surface characteristics and gravitation [17]. Terrestrial applications include off-road vehicles for military and search & rescue functions. In a general sense, terrain is classified as "rough" and/or "challenging" as characterized by its progressive rock density, its variable, unpredictable surface properties (e.g., sandy, frangible, soft-dust-penetrable, icy), and steepness. Terrainability and traversability of mobile robots must be considered in context of scale and design. Our report here

addresses wheeled vehicles; other options exist including legged, tracked, modular-articulated, and less conventional uni-and-multiwheeled inflatable systems. Each have their respective strengths relative to particular domains and ranges of application—e.g., hard versus soft soil floatation properties, speed versus size, traversability relative to obstacle density and control complexity. Rover scale relative to terrain roughness, obstacle frequency, and obstacle size distribution also sets design constraints and performance criteria. E.g., smaller vehicles benefit from cube-square law effects (power, floatation), while larger vehicles finesse obstacles and rocky traverses by mechanical advantage. In summary, planetary mobility is a set of design trades between mechanical complexity/robustness, mass/volume/power resources, and computationally practical perception/control/planning that can detect, classify and mitigate obstacles and anomalies (as well as capture and maintain the necessarily accurate on-board, real-time model of vehicular state with respect to the surrounding terrain, examples being localization, pose, and wheel-soil interaction parameters). Planetary rovers are often quite limited in mass/volume/power resources and to date are largely of conventional wheeled design (Cf., rocker-bogie mechanization of NASA/JPL's MPF-Sojourner '97 and MER/'03 vehicles, which have near optimal obstacle clearance for a six wheel form factor).

We have organized our research around four related themes, and surveyed prior related work in refs. [6, 12]: 1) physics-based mobility models for robust terrain traverse/interactions; 2) computationally-efficient, behavior-based control architectures that exploit these models; 3) rover designs having actively controlled, reconfigurable elements that improve agility/stability of traverse; and 4) extension of these concepts into networked and modular robotic systems that exploit collective estimation, distributed control, and coordinated multi-agent behaviors to perform tasks of larger, more complex scale.

2. Rover-Terrain Interactions

In this section we overview our recent development of models for terrain interaction. Terramechanics, while a long studied subject, appears to be a fairly new research topic in rover design, possibly due to rather wide-ranging surface characteristics, the non-linear underlying wheel interactions, and empirical testing requirements. Better wheel-terrain interaction models—both their on-line identification and predictive estimation—will enable power-efficient rover operation, fault diagnosis, and related contingency handling (wheel sinkage, vehicle slewing, etc.). It will also lead to new scientific tools for inference of planetary surface analysis and characterization.

2.1. Problem Background and Statement

Wheel-terrain interaction has been shown to play a critical role in rough-terrain vehicle mobility [1, 18]. However, modeling and identification of such phenomena is often overlooked in robotic applications, possibly because methods for terrain parameter identification require costly and dedicated testing equipment. For planetary rovers, it would be desirable to estimate terrain physical parameters on-line, since knowledge of a terrain region's physical parameters would enable a rover to accurately predict its traversability and adapt its *in situ* control and planning strategy [5]. Finally, terrain parameter estimation employs rovers in new ways for improved scientific understanding of planetary composition, per [8].

Many parameters are required to fully describe a terrain's mechanical characteristics, including cohesion, internal friction angle, shear deformation modulus, pressure-sinkage moduli, etc. Two key terrain parameters are cohesion, c , and internal friction angle, ϕ . These parameters can be used to compute the maximum terrain shear strength, τ_{max} , from Coulomb's equation:

$$\tau_{max} = c + \sigma_{max} \tan \phi \quad (1)$$

where σ_{max} is the maximum normal stress acting on a terrain region. Since soil failure occurs when the maximum shear strength is exceeded, knowledge of c and ϕ can be used to predict rover traversability. Note that c and ϕ are also well-established scientific parameters for characterizing soils.

We outline a method for on-line estimation of terrain cohesion and internal friction angle using on-board rover sensors. The algorithm estimates parameters of terrain the rover is currently traversing. The algorithm relies on a simplified form of classical terramechanics equations, and uses a linear-least squares estimator to compute terrain parameters in real time. The method is computationally efficient, and is thus suitable for implementation on a rover with limited on-board computing resources.

2.2. Technical Approach

A free-body diagram of a driven rigid wheel traveling through deformable terrain is shown in *Figure 1*. Nonlinear force balance equations can be written for the system in Figure 1, relating stresses at the wheel-terrain interface to externally applied force such as the wheel weight and torque [1]. A key insight of our approach is to approximate the nonlinear force equations by simplified linear forms. The linearized force balance equations can be solved for the terrain parameters c and ϕ . Details of this approach are presented in [7].

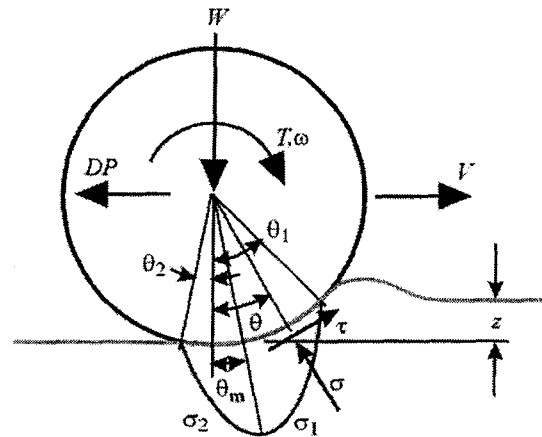


Figure 1: Rigid wheel on deformable terrain

Inputs to this estimation method are the wheel load, torque, slip, and sinkage. All of these quantities can be measured or estimated for a rover moving at slow speeds. The load can be computed from a quasi-static force analysis of the rover. The torque can be estimated from the current input to the motor and an empirically-determined mapping from current to torque. The wheel angular speed can be measured with a tachometer, and the

linear speed can be computed using IMU measurements. The wheel sinkage can be computed from vision-based techniques that have been recently developed at MIT, per *Figure 2*.

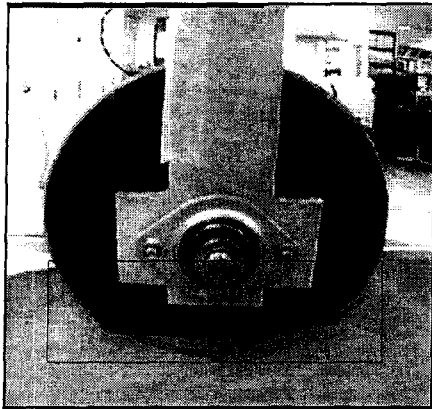


Figure 2: Vision-based estimate of wheel sinkage

2.3. Results

Extensive simulations and experiments have been performed to validate the terrain parameter estimation algorithm. Representative results are shown in *Figure 3*.

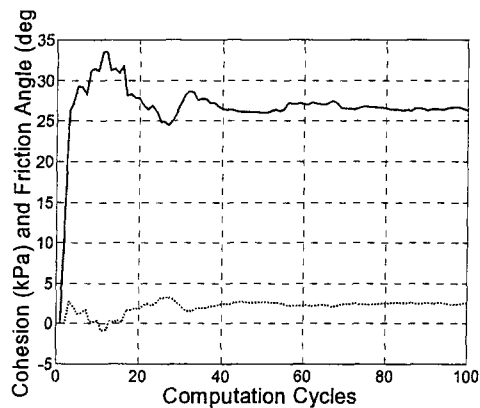


Figure 3 (a): Simulation—estimation of cohesion (solid) and internal friction angle (dotted)

Figure 3a is a simulation of a single wheel traveling through sandy terrain. Sensor noise and wheel dynamics are included in the simulation. It can be seen that the estimated parameters c and ϕ quickly converge to the true values of $c = 2.0$ and $\phi = 27.0$.

Figure 3b presents experimental results from an instrumented wheel testbed developed at MIT. Here the wheel is traveling through dried bentonite clay. Again, it can be seen that c and ϕ quickly converge to near the measured values of $c = 0.7$ and $\phi = 32.1$.

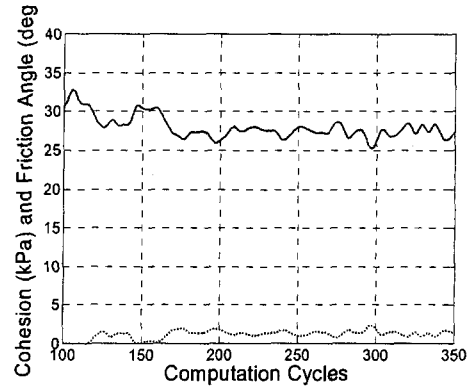


Figure 3 (b): Experiment—estimation of cohesion (solid) and internal friction angle (dotted)

2.4. Current Directions of Research

Our continued investigation of rover-terrain interactions and related terramechanical modeling proceeds along two distinct directions: nonparametric traversability prediction, and “visual terrain association”. In non-parametric traversability, the goal is to predict the immediate vehicular mobility properties by conducting a simple on-line “experiment”, such as quickly spinning a wheel. Such an approach would not explicitly estimate terrain parameters; rather it would yield a rapid estimate of traversability. In visual terrain association, our further goal is to use on-board processed visual cues so as to correlate previously sensed terrain with that next to be traversed. Having this sort of capability would enable a rover to develop a terrain-based traversability map of its surroundings, which would be a valuable aid to higher level motion planning functions.

3. Traversal of Challenging, Steep Terrain

In this section we first describe a reconfigurable rover that adapts its kinematics pose and c. g. distribution for stable traverse over changing terrain slope up to 50 degrees. We then present a cooperative rover system for access of cliffs.

3.1. Problem Background and Statement

Increased rover autonomy is required for long duration robotic presence on lunar and planetary surfaces. This need is being addressed by a number of ongoing research programs, with emphasis on accurate, safe long-range autonomous navigation traverse and automated science instrument placement [2, 14]—functions that increase the science return per unit time of operations, while also reducing ground support requirements. Such planetary rover operations have to date been in the context of low rock density terrains typified by Viking 1 and Mars nominal imagery—6-to-9% area density, and small scale rock outliers. Beyond this regime, approaching Viking 2 densities of 18 % and larger rocks, wheeled rovers of current scale (1 meter² length/track) confront problems of trapping, mean-free path obstruction, and in absence of robust sensing and hazard avoidance planning, also the risk of mission catastrophic upsets (by both positive and “negative” obstacles, that is, surface depressions). Thus, there is motivation to not only map and locally plan [2, and references therein] for obstacle avoidance, but also to enhance rover traverse capability by mechanical and sensory-control adaptation. Desired improvements are both quantitative and qualitative—rovers that drive more robustly through more variable VL1/VL2 Mars terrain, and new rover systems able to access increasingly difficult, steeply sloped regions of science importance. *Figure 4* gives two examples of recent note in the space science community; it is hoped these sites will afford a rich developmental history of their formative processes through exposed strata of highly sloped terrains.

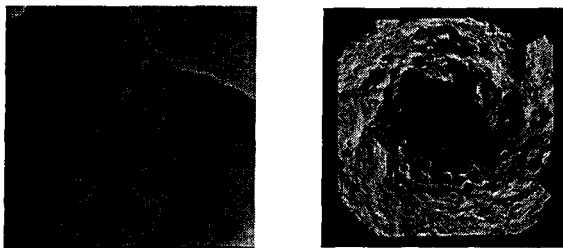


Figure 4: Examples of very challenging terrain of great scientific importance—(left) Mars cliff-face with signs of water outflows, observed by Mars Odyssey orbiter (2001), (right) Lunar South Pole-Aitken Basin where signs of water were found by Clementine and Lunar Prospector

Future rover solutions to “high risk access” will likely include both single and multiple robot systems, as we subsequently illustrate. In the latter regard, rover “crews” are expected to play important roles not only in planetary exploration, but also in preparing/maintaining habitats for robotic and teamed human/robotic presence [13, 14].

3.2. “All Terrain Explorer” Development

Figure 5 sketches our concept and representative operational scenarios that motivate it. In one element of our technical approach [12], the rover images its forward-looking terrain, derives from on-board stereo a 3D terrain map, analyzes terrain traversability relative to predicted kinematic-and-quasistatic maneuverability/stability, and sequences compensating behaviors that optimize a rover performance index. These behaviors are sequenced by a simple finite state machine on JPL’s Sample Return Rover, reposing stance and c.g. This is done in two ways: by independent articulation of the rover shoulder strut angles, and by repositioning of the rover top-mounted robot arm. Per *Figures 5 and 6*, the arm is a reconfigurable resource for use in both kinematically unconstrained and closed-loop fashions. In the latter case (as yet un-implemented), the arm acts as a drive actuator, pivot point, or other element in its rover-ground interactions (“de-trapping”, stabilization, anchoring, etc.).

Posture and Mobility Modes	Center of Gravity Reposition	Shoulder Repose/Lower	Arm Ground Contact	“Body Over”	“Climbing”	Joint Shift or Locking
Detectable Predictable Conditions						
Traction Loss	Wheel Obstacle & Wheel Contact				Wheel Obstacle & Wheel Contact	
Steep Slope	Arm Positioning & Stability	Roll/Tilt/Slump & Pump Trip		Steep Slope	Roll/Tilt/Slump & Wheel Contact	
Wheel Trap			Wheel Contact			
Support Load			Arm/Shoulder/Tail Swing			Arm/Shoulder/Tail Swing
Obstacle						Wheel Trip
Tip Over			Roll/Tilt/Slump			

Figure 5: Trigger Conditions for Rover Reconfiguration

We do not incorporate rover dynamics, as they are not a contributory factor relative to the 5-to-10 cm/sec traverses we are addressing. We incorporate static friction-and-slip effects in the above predictive JPL algorithm, treating these through kinematics/quasistatics analysis referred to surface contact models and an idealized Coulomb friction model. Complementing this *predictive approach* to rover reconfiguration, we utilize a *reactive approach* developed

by MIT with JPL [6] wherein rover stability analysis is based on instantaneous state (engineering sensor data as to pose and articulation) and physically based planning. This technique is very computationally efficient. We next briefly describe these two algorithms.

Predictive reconfiguration: In summary, we predict the future state of the rover based upon look-ahead stereo range imaging, on-board IMU, and any other derived state information that can be sensed, e.g., stall conditions, inferred slip from accelerometry, etc. This information is used to compute a tipover-stability and slip-and-traction *Locomotion Metric* that determines feasible and appropriate reconfiguration of rover geometry and center-of-mass. The algorithmic procedure is [12]:

1. Determine the surface shape of terrain ahead of the rover (model by appropriate spatial representation).
2. Solve the configuration kinematics to predict rover configuration on the modeled terrain, i.e. roll, pitch, yaw, internal angles, and wheel contact points
3. Given a friction coefficient that characterizes wheel-ground interactions, determine if the span of nominal frictional and normal forces at the predicted contact are sufficient to resist the *gravity wrench* (and any other disturbance forces) in both the nominal and re-configured kinematics/c.g. (Reconfiguration consists of independent left-right shoulder angle changes and center-of-gravity shifts using the manipulator).
4. Determine the minimum coefficient of friction in Step 3. This term is interpreted to be a *Locomotion Metric* indicative of the quality of the given configuration (or reconfiguration).

Step 1 is implemented by stereo imaging—correlating Laplacian left and right images along epi-polar lines to establish image disparity, and consequently the range, via a camera model. Step 2 is computed by means of an iterative Newton Solver. Step 3 involves setting up polyhedral inequality approximations to the friction cone at each rover contact point, and expressing as inequalities the unidirectional constraints on the wheel normal forces and the wheel torque constraints. These linear relationships are then transformed to the vehicle frame using the vehicle *Locomotion Matrix* [12, and refs. therein]. An equality constraint characterizes the manifold of contact forces able to resist the applied wrench without regard to

constraints. A linear programming solution uses these inequality and equality constraints to determine if a feasible set of friction and normal forces exists to resist the applied wrench. A binary search algorithm then computes the metric by determining the smallest value of friction coefficient sufficient to resist the applied vehicle wrench.

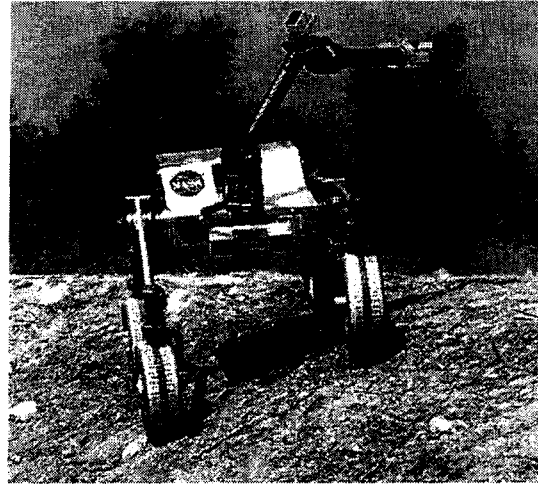


Figure 6: SRR (<http://prl.jpl.nasa.gov>) descends a steep hill at the Arroyo Seco near JPL. By comparison to operation with fixed shoulder and arm in stowage, slope access stability more than doubles, from ~20+ degrees up to 50.

Reactive reconfiguration: We define a stability metric using a quasi-static model and optimize this metric on-line. Our method relies on estimation of wheel-terrain contact angles as derived from simple on-board sensors alone. As the rover moves at 5-to-6 cm/sec, we consider only static forces in calculating the rover stability. System stability is expressed in terms of a set of “stability angles.” A stability angle is the angle formed between a line originating at the center of mass and normal to the tip-over axis, and the gravitational (vertical) axis. This angle goes to zero at marginal stability. A performance index, Φ , is defined for the SRR from these stability angles γ_i , $i=\{1,\dots,4\}$, and the reconfigurable shoulder degrees of freedom, ψ_1 and ψ_2 , as *Equation 2* [6]

$$\Phi = \sum_{j=1}^4 \frac{K_j}{\gamma_j} + \sum_{i=1}^2 K_{i+4} (\psi_i - \psi'_i)^2 \quad (2)$$

where K_i and K_j are positive constants and the stability angles γ_j are functions of the shoulder and

manipulator degrees of freedom (i.e. $\gamma = \gamma(\psi_1, \psi_2, \theta_1, \theta_2, \theta_3)$). Note that the first term of Φ tends to infinity as the stability at any tip-over axis tends to zero. The second term penalizes deviation from a nominal configuration of the shoulder joints, thus maintaining adequate ground clearance, an important consideration in rough terrain. The goal of this stability-based optimization problem is to minimize the performance index Φ subject to joint-limit and interference constraints. For rapid computation, and due to the simple nature of Φ , we can employ a basic optimization technique such as conjugate-gradient search. Overall, the approach is computationally effective, does not require visual terrain knowledge, and treats gravitational versus traction issues.

3.3. "Cliff-bot" Cooperating Rover System

Clementine and Lunar Prospector mission imagery indicate presence of water in the Lunar Aitken Basin at the south lunar pole. Mars Odyssey orbital imagery infer recent, possibly active water outflows in steeply cratered regions. There is thus very strong motivation to develop planetary mobility systems that can access designated science targets on cliff-like slopes, per *Figure 7*, a topic for which JPL has developed a recent technical proof of concept around a cooperating multi-robot system. We briefly overview our approach, as described in more detail elsewhere [3, 4, 9 and references therein]. In *Section 4*, we overview more recent related MIT/JPL work on fused sensing in support of this "Cliff-bot" system concept.

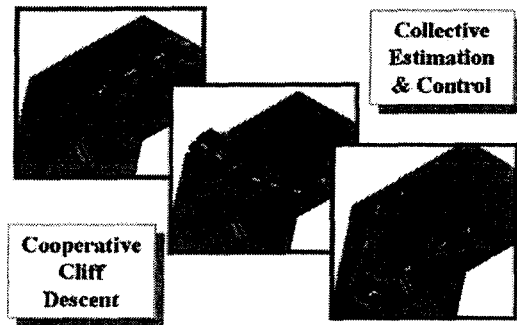


Figure 7: Concept—multiple, modular, cooperative and re-taskable robots reconfigure and tightly coordinate their sensing and control in a cliff descent for scientific analysis of exposed stratigraphy (geo-morphology, bio-chemistry)

The Cliff-bot, *Figure 8*, employs two anchored rover analogs as "anchor-bots" topside of the cliff. These anchor-bots fully implement the kinematics controls and degrees-of-freedom of the two robots they emulate. The conceptual system, per *Figure 7*, is based in a modular ensemble of robots that reconfigures itself at the top of the cliff, first anchoring two members at the top, then sending a tethered robot over the cliff-edge onto the cliff-face. The "tether-bot" actively drives/traverses the cliff-face using way-point navigation, with stability being maintained by actively controlled tethers from the two anchor-bots.



Figure 8: Cliff-bot way point navigation on a cliff face via active tether-bot driving and cooperative tether control with two topside two anchor-bots

The Cliff-bot system is implemented in JPL's recently developed *CAMPDOUT* architecture, per *Figure 9*.

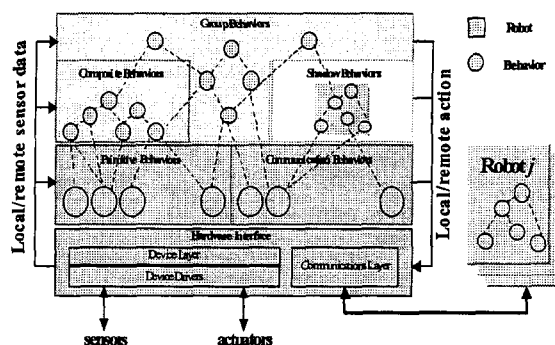


Figure 9: JPL *CAMPDOUT* high-level organization for collective sensing and tightly coordinated control within extensible multi-robot networks [4, 10, 11]

Within space limitations, we sketch Cliff-bot control per a behavior network shown for one of the anchor-bots in *Figure 10*. See reference [4] for more detail. Behavior composition of Cliff-bot within CAMPOUT employs a priority weighting of four primary behaviors: *Stability*, *Maintain Tension*, *Match Velocity*, and *Haul*. *Stability* is given the highest priority, as it minimizes the risk of rover tip-over; *Maintain Tension* keeps constant tension on the tethers; *Match Velocity* controls tether payout rates to match those of the active agent on the cliff face; and *Haul* gives the active agent a pull if it has insufficient torque to get moving at the start of a traverse. All state data is shared between the modules by means of a publish-and-subscribe communication protocol.

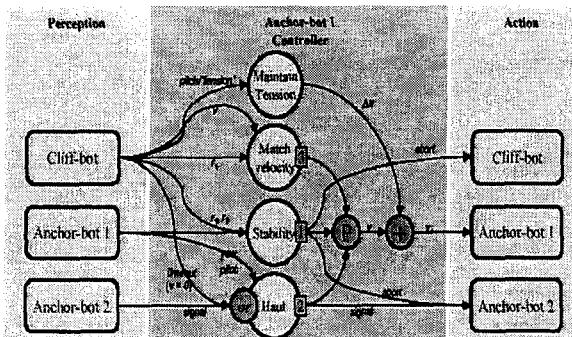


Figure 10: Subset of the behavior network for collective cliff-descent illustrating a sub-system for controlling the velocity of anchor-bot 1. The arrows represent data links between local blocks as well as remote components (e.g., behaviors, sensors, actuators)

Utilizing the general scheme above, we have successfully used Cliff-bot to traverse rocky soil inclines of 55-to-80 degree slope. In the absence of stabilizing tether control, including detection of tether obstruction, the deployed cliff rover is often unstable at inclines < 25 degrees (note that the tether-bot is operated here as a fixed configuration vehicle, unlike the All Terrain Explorer of *Section 3.2*).

4. Cliff-bot Perception & State Estimation

The prior Cliff-bot discussions did not address the issue of perception—the development of a fused state estimate of the external/internal environment to explicitly support navigation and planning of the tether-bot. Here we do so.

4.1. MITSAF Algorithm and Implementation

Sujan [16] recently developed an algorithm that fuses sensory information from multiple robotic agents. His approach exploits physical sensor, robot, and environmental models to yield geometrically consistent surrogate information in lieu of missing data (thereby reducing uncertainty in the overall system state). A central concept within the algorithm is sensor planning: efficient and iterative re-positioning of sensors using an information theoretic optimizing criteria. Thus sensor positions are planned to help fill in uncertain/ unknown regions of the environment model. Sensory information obtained from this process is distributed to the agents. The key idea of the algorithm is to build a common environment model by fusing the data available from the individual robots, providing both improved accuracy as well as knowledge of regions not visible by all robots. As pertains to prior JPL Cliff-bot system development and demonstration [9], MITSAF utilizes an additional “RECON-bot” (REmote Cliff Observer and Navigator) that serves as a mobile observer/ sensing module, per *Figure 11*.

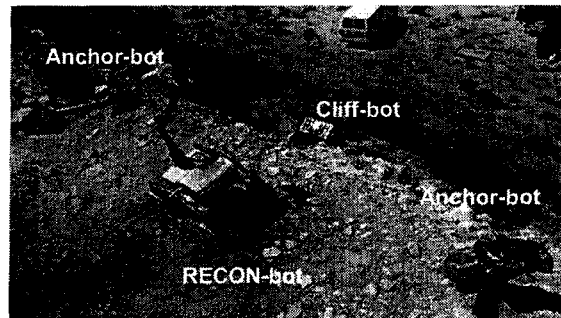


Figure 11: Cooperative cliff descent system, consisting of two anchor-bots, cliff-bot, and a RECON-bot, the last of which surveys cliff face from the top edge, and passes the path for a chosen goal to the tether-bot

The four robots are equipped with a limited sensor suite, computational power and communication bandwidths. The tether-bot—which in actual planetary science practice would serve primarily to transport and position a science payload—has minimal resources for navigation beyond the essential. By complement, the RECON-bot observes the global environment traversable by the tether-bot and communicates to it key navigational data. While tether-bot can carry cameras and other onboard sensors

for local observations, its independent sensor view space, sensor placement, self-localization and navigational planning are severely constrained by surrounding rocks, larger outcroppings, etc. Further, there is significant task uncertainty in relative pose between the multiple robots and the environment model. Given these limitations and underlying uncertainties, classical robot control and planning techniques break down. In essence, it is difficult or impossible to directly measure the environment model required for the control of interacting cooperative mobile field robots. The new **MITSAF** (**M**odel-based **I**nformation **T**heoretic **S**ensing **A**nd **F**usion) algorithm addresses the preceding issues as follows:

1. *System initialization*: This step involves initializing the environment map, localizing robots, and generating a first map. Here, we map the environment to a 2.5D elevation grid, i.e. each grid cell value represents the average elevation at that cell. Next, robots contributing to or requiring use of the environment model are localized with respect to the initial environment map. Finally, initial environment sensing is performed.

2. *Critical terrain feature identification*: In several applications, certain regions in the terrain may be task critical and require prior identification/modeling. For example, unique to this application, the cliff edge requires identification by the RECON-bot. This edge is parameterized by the edge of a best-fit non-convex polygon of the local terrain. This permits the RECON-bot to traverse a geometrically complex cliff edge without falling over while not committing large memory/processing time resources.

3. *Optimum information gathering pose selection*: The planner selects new vision sensor positions for the agents contributing sensory data to the environment model. In this application this is limited to the RECON-bot. A rating function is used to determine the next pose of the camera from which to look at the unknown environment. The aim is to acquire the maximum new information of the environment that would lead to a more complete environment map. Specifically, the new information (H , to be next discussed) is equal to the expected information of the unknown/partially known region viewed from the camera pose under consideration. This is based on known obstacles from the current environment model, the field of

view of the camera and a framework for quantifying information. Shannon [15] has shown that the information gained by observing a specific event among an ensemble of possible events may be described as follows:

$$H(q_1, q_2, \dots, q_n) = -\sum_{k=1}^n q_k \log_2 q_k \quad (3)$$

where q_k represents the probability of occurrence for the k^{th} event. This definition of information may also be interpreted as the minimum number of states (bits) needed to fully describe a piece of data. Shannon's emphasis was in describing the information content of 1-D signals. As shown before, it is possible to extend this formulation of information to a generalized 3-D signal [16]. As reported here, the idea is in fact applied to a 2.5D signal—the environment elevation map. *The new information content for a given camera view pose is given by:*

$$H(\text{cam}_{x,y,z,\theta_p,\theta_y}) = \sum_i \frac{n_{\text{grid}}^{\text{max}} - n_{\text{grid}}^i}{n_{\text{grid}}^{\text{max}}} \left\{ \begin{aligned} &\left(\frac{P_v^i}{2} \log_2 \frac{P_v^i}{2} \right) \\ &+ \left(1 - \frac{P_v^i}{2} \log_2 \left(1 - \frac{P_v^i}{2} \right) \right) \end{aligned} \right\} \quad (4)$$

where H is summed over all grid cells, i , visible from camera pose $\text{cam}_{x,y,z,\theta_p,\theta_y}$; n_{grid}^i is the number of environment points measured and mapped to cell i ; $n_{\text{grid}}^{\text{max}}$ is the maximum allowable mappings to cell i ; and

P_v^i is the probability of visibility of cell i from the camera test pose. The above formal definition of information behaves in an intuitively correct way: Regions with higher visibility and/or a higher level of associated unknowns yield a higher expected information value. Conversely, areas of higher occlusion or better known regions result in lower expected information values.

4. *Model distribution*: As the environment model is developed it needs to be distributed among the agents so that optimum sensor placement planning may continue. The environment model distribution is also required for task execution. For example, after the RECON-bot has developed the geometrical cliff surface model, it needs to

transfer this data to the Cliff-bot for the latter's science instrument placement/observational positioning function. We have developed a data transfer procedure that reflects practical inter-rover communication bandwidth limits. The underlying data reduction algorithm breaks down the environment map (data set) into interest regions using a quad-tree. This is done by first reducing the elevation map with adaptive decimation which removes objects insignificant to the Cliff-bot wheel diameter. The resulting data set is divided in four quads and each is evaluated for information content, per the criteria of *Equations 3 and 4*. This outcome is used to determine if further quad-subdivision (higher resolution) is required. If not, then an average elevation value of the particular quad is used for transmission (rather than the elevation of all grid cells within the quad). This results in a significantly reduced data set. Conventional compression schemes may then be applied to the reduced data set to further reduce the number of transmission bits.

4.2. Experimental Results

We have described JPL's development of an integrated Cliff-bot perceptual system and use therein of MITSAF in [3, and refs. therein]; Cliff-bot builds on several recent JPL rover R&D efforts, in particular, the autonomous perception and navigation algorithms of FIDO rover [2, 14]. Here, we show illustrative results of collaborative JPL-MIT Cliff-bot experimentation with MITSAF.

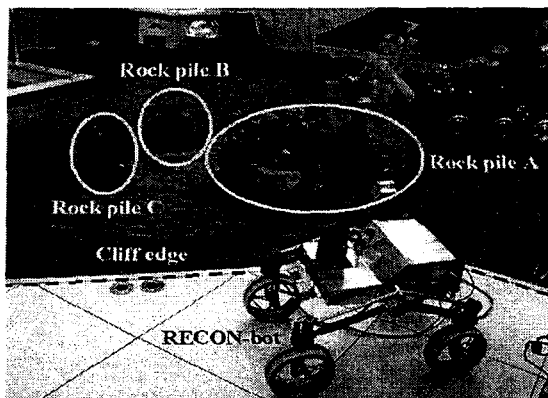


Figure 12: Experimental setup in JPL PRL with SRR as a RECON-bot, three rock piles, and a small step edge (marked with dotted lines) serving as the cliff-edge

We conducted our experimental tests in the *Planetary Robotics Laboratory (PRL)* at JPL, <http://prl.jpl.nasa.gov> and in the field at a cliff-site near the Tujunga Dam in Tujunga, CA. We show the experimental set-up for lab study in *Figure 12*, wherein the Sample Return Rover (SRR, a JPL technology prototype (as earlier described in its Section 3 role as the "All Terrain Explorer", acts as the RECON-bot. The SRR is a four-wheeled mobile robot with independently steered wheels and independently controlled shoulder joints; SRR carries stereo cameras (15cm baseline, the individual cameras having a 45° field-of-view) mounted on its four degree-of-freedom manipulator, which also functions as a steerable mast. As applies to this study, SRR computing includes a 266 MHz Pentium II processor in a PC-104+ stack that operates under the real-time OS VxWorks5.4. We implemented five mapping techniques with increasing levels of sophistication, per *Figure 13*: raster scanning without yaw, raster scanning with yaw, information-based environment mapping with the cliff edge assumed to be a straight line segment, information-based environment mapping with the cliff edge approximated as a non-convex polygon, and information-based environment mapping with interest function and cliff edge approximated as a non-convex polygon. The first two methods reflect common environment mapping schemes. The latter three methods reflect, with increasing model and computational complexity, the MITSAF algorithm. Laboratory and field tests (*Figures 12 and 11*) both confirm the effectiveness of MITSAF.

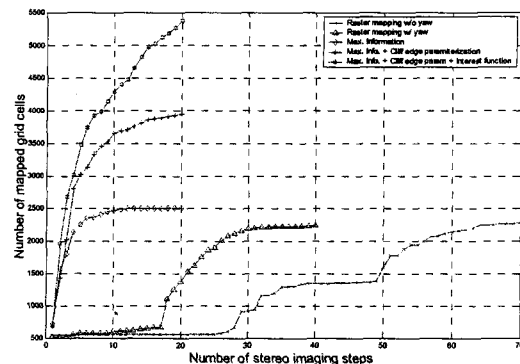


Figure 13: Five lab studies of Cliff-bot environmental mapping, wherein the upward trend reflects increasing fidelity/coverage per the five listed techniques (see text)

Acknowledgments

The research described in this paper was carried out at the Jet Propulsion Laboratory, California Institute of Technology, under a contract with the National Aeronautics and Space Administration. The portion of this work done by MIT is supported by NASA/Jet Propulsion Laboratory under contract number 1216342.

References

- [1] G. Bekker, *Introduction to Terrain-Vehicle Systems*, University of Michigan Press, 1969.
- [2] T. Huntsberger et al., "Rover Autonomy for Long Range Navigation and Science Data Acquisition on Planetary Surfaces," Proc. 2002 IEEE Intl. Conf. on Robotics and Automation, Washington, D.C.
- [3] T. Huntsberger, V. A. Sujan, S. Dubowsky, and P. S. Schenker, "Integrated System for Sensing and Traverse of Cliff Faces," in Proc. SPIE Aerosense, Vol. 5083, April 22-24, 2003.
- [4] T. Huntsberger et al., "CAMPOUT: A Control Architecture for Tightly Coupled Coordination of Multi-Robot Systems for Planetary Surface Exploration," in *IEEE Trans. on Systems, Man, & Cybernetics: Spec. Issue on Collective Intelligence*, 2003.
- [5] K. Iagnemma and S. Dubowsky, "Mobile Robot Rough-Terrain Control (RTC) for Planetary Exploration," in Proc. 26th ASME Biennial Mechanisms and Robotics Conf., DETC 2000, 2000.
- [6] K. Iagnemma, A. Rzepniewski, S. Dubowsky, P. Pirjanian, T. Huntsberger, and P. Schenker, "Mobile robot kinematic reconfigurability for rough-terrain," in Proc. SPIE Sensor Fusion and Decentralized Control in Robotic Systems III, Vol. 4196, 2000; and, K. Iagnemma, A. Rzepniewski, S. Dubowsky, and P. Schenker, "Control of Robotic Vehicles with Actively Articulated Suspensions in Rough Terrain," *Autonomous Robots*, 14, pp. 5-16, 2003.
- [7] K. Iagnemma, H. Shibly, and S. Dubowsky, "On-Line Terrain Parameter Estimation for Planetary Rovers," *ibid.* [2].
- [8] J. Matijevic et al., "Characterization of Martian Surface Deposits by the Mars Pathfinder Rover, Sojourner," *Science*, Volume 278, Number 5, pp. 1765-1768, 1997.
- [9] P. Pirjanian et al., "Distributed Control for a Modular, Reconfigurable Cliff Robot," *ibid.* [2].
- [10] P. Pirjanian et al., "CAMPOUT: A control architecture for multirobot planetary outposts," in Proc. SPIE Conf. Sensor Fusion & Decentralized Control in Robotic Systems III, 4196, pp. 221-230, 2000.
- [11] P. Pirjanian, T.L. Huntsberger, and P. S. Schenker, "Development of CAMPOUT and its further applications to planetary rover operations: A multirobot control architecture," in Proc. SPIE on Sensor Fusion & Decentralized Control in Robotic Systems IV, 4571, pp. 108-119, 2001.
- [12] P. S. Schenker, P. Pirjanian, B. Balaram, K. S. Ali, A. Trebi-Ollennu, T. L. Huntsberger, H. Aghazarian, B. A. Kennedy, E. T. Baumgartner, K. Iagnemma, A. Rzepniewski, S. Dubowsky, P. C. Leger, D. Apostolopoulos, and G. T. McKee, "Reconfigurable robots for all terrain exploration," *ibid.* [10], and references therein.
- [13] P. S. Schenker, T. L. Huntsberger, P. Pirjanian, A. Trebi-Ollennu, H. Das, H., S. Joshi, H. Aghazarian, A. J. Ganino, B. A. Kennedy, and M. S. Garrett, "Robot work crews for planetary outposts: close cooperation and coordination of multiple mobile robots," *ibid.* [12].
- [14] P. S. Schenker et al., "Planetary rover developments supporting Mars science, sample return and future human-robotic colonization," *Autonomous Robots*, 14, pp. 103-126, 2003.
- [15] C. E. Shannon, "A mathematical theory of communication," *The Bell System Technical Journal*, vol. 27, pp. 379-423, July, 1948.
- [16] V.A. Sujan and S. Dubowsky, "Visually Built Task Models for Robot Teams in Unstructured Environments," *ibid.* [2]; and, V. A. Sujan, *Compensating for Model Uncertainty in the Control of Cooperative Field Robots*, Ph.D. Thesis, Dept. of Mech. Eng., MIT, Cambridge, MA., June 2002.
- [17] Mark V. Sykes (Ed.), *The Future of Solar System Exploration, 2003-2013*, NRC Planetary Decadal Report, 2002 (<http://www.aas.org/~dps/decadal>).
- [18] J. Wong, *Terramechanics and off Road Vehicles*, Elsevier, 1989.